Chemical Bond and Charge Transfer Dynamics of a Dye-Hierarchical TiO_2 Hybrid Interface

Journal:	*The Journal of Physical Chemistry*
Manuscript ID:	jp-2014-125734.R2
Manuscript Type:	Article
Date Submitted by the Author:	24-Mar-2015
Complete List of Authors:	Castellarin-Cudia, Carla; IOM-CNR Laboratorio TASC, Caruso, Tommaso; Università della Calabria, CNISM-Dipartimento di Fisica Maccallini, Enrico; Università della Calabria, CNISM-Dipartimento di Fisica Li Bassi, Andrea; Politecnico di Milano, Department of Energy Carrozzo, Paolo; Politecnico di Milano, Department of Energy De Luca, Oreste; Università della Calabria, CNISM-Dipartimento di Fisica Goldoni, Andrea; Elettra-Sincrotrone Trieste S.C.p.A., Lyamayev, Victor; Institute of Electron Physics, Prince, Kevin; Elettra-Sincrotrone Trieste, Bondino, Federica; IOM-CNR Laboratorio TASC, Magnano, Elena; Sincrotone Trieste, ; IOM-CNR Laboratorio TASC, Agostino, Raffaele; Università degli Studi della Calabria, Fisica Casari, Carlo Spartaco; Politecnico di Milano, Department of Energy

Chemical Bond and Charge Transfer Dynamics of a Dye-Hierarchical TiO_2 Hybrid Interface

Carla Castellarin-Cudia[a,b], *Tommaso Caruso*[c,] ***, *Enrico Maccallini*[c] , *Andrea Li Bassi*[d,e], *Paolo Carrozzo*[d,e], *Oreste De Luca*[c], *Andrea Goldoni*[a], *Victor Lyamayev*[a,f], *Kevin Charles Prince*[a,b], *Federica Bondino*[b], *Elena Magnano*[b], *Raffaele Giuseppe Agostino*[c], *Carlo Spartaco Casari*[d,e]

[a]Elettra-Sincrotrone Trieste S.C.p.A. s.s.14 km. 163.5, I-34149 - Trieste, Italy

[b]Istituto Officina dei Materiali-CNR, Laboratorio TASC, s.s.14 km. 163.5 I-34149 - Trieste, Italy

[c]CNISM-Dipartimento di Fisica, Università della Calabria, Ponte Bucci, Cubo 33c, I-87036 Arcavacata di Rende (Cs), Italy

[d]Dipartimento di Energia and NEMAS-Center for Nano Engineered Materials and Surfaces, Politecnico di Milano, Via Ponzio, 34/3 I-20133 Milano, Italy

[e]Center for Nano Science and Technology @Polimi, Istituto Italiano di Tecnologia, Via Pascoli 70/3, 20133 Milano, Italy

[f]European XFEL GmbH, Notkestraße 85, 22607, Hamburg, Germany

Corresponding Author * email: Tommaso.caruso@fis.unical.it, phone: 0039-(0)984-496095

Abstract

The adsorption of Zn-Tetra-Phenyl-Porphyrin (ZnTPP) on nanoporous hierarchically organized anatase TiO_2 structures, and the properties of the corresponding hybrid interface were studied by synchrotron radiation experiments. The molecular structure, electronic properties and the bonding with nanostructured TiO_2 surfaces were analyzed by photoemission (XPS and UPS) and x-ray absorption spectroscopy (XAS). The charge transfer at the interface was investigated by means of valence band resonant photoemission experiments (ResPES) at the C K edge. We show that the charge transfer dynamics between the photo-excited ZnTPP and TiO_2 is strongly influenced by the presence of defects on the TiO_2 surface. On a stoichiometric anatase nanostructure, ZnTPP bonding occurs primarily via carbon atoms belonging to the molecular phenyl rings and this creates a preferential channel for the charge transfer. This phenomenon is reduced in the case of defective TiO_2 surface, where ZnTPP interacts mainly through the molecule macrocycle. Our results represent a surface science study of the dye molecule behavior on a nanoporous TiO_2 photoanode relevant to dye-sensitized or hybrid solar cell applications and it shows the importance of the surface oxidation state for the charge transfer process.

Keywords: dye adsorption, titanium dioxide, resonant photoemission, x-ray absorption, photovoltaic, Graetzel's cell.

1. Introduction

Hybrid interfaces formed by organic molecules interacting with inorganic surfaces, such as metals or oxides, are attracting increasing interest for their fundamental role in novel devices, like solar cells, sensors, nanoelectronic and optoelectronic components. In dye-sensitized solar cells (DSSCs) light is absorbed by a dye molecule, the electron-hole pair is separated at the interface with the inorganic surface and the electron is injected into a TiO_2 photoanode[1-2]. The DSSC device performance is strongly dependent on the efficiency of charge separation and on fast electron injection into the oxide. In turn, such phenomena are related to the complex interaction at the nano-molecular scale between the dye molecule and the oxide surface.

To this respect the behavior of novel components is of great importance to assess the interest of new solutions for DSSC technology, comprising alternative dye molecules as well as innovative nano- and meso- photoanode architectures.

For example, by employing a customized zinc-porphyrin molecule in conjunction with a cobalt (II/III) redox electrolyte instead of the usually employed ruthenium-dyes and iodide/triiodide redox couple, a very high DSSC efficiency (12%) was obtained by M. Graetzel's group[3]. Morevoer, photoanodes are typically made from micrometer thick nanoparticle aggregates with high specific surface area. One-dimensional structures such as nanotubes, nanowires and nanorods of TiO_2 and ZnO were tested as possible alternatives[4-7], with the aim of exploiting preferential vertical transport path for the electrons and the possibility of light trapping/harvesting through proper management of light scattering. Recently, quasi 1D structures consisting of TiO_2 clusters hierarchically assembled in open-porous mesostructures resembling a forest of nano-trees were fabricated and tested in DSSCs, showing improved electron lifetime and electrolyte diffusion[8-9] and in solid state DSSC, showing improved performance due to light trapping effects related to a hyperbranched morphology[10].

More generally, porphyrins are attracting a lot of interest, among other molecular systems, for their overall properties. They are a vast family of molecules, which play an important role in biological systems[11-12] and their base structure consists of a macrocycle core, i.e. four pyrrole groups interconnected by meso-bridge carbon atoms, and several terminal groups attached externally to the core macrocycle. Accompanied by redox reactions, many metals can be inserted in the macrocycle center forming metallo-porphyrins. They efficiently absorb light in the visible range, showing electronic and adsorption properties on surfaces that can be tuned by modifying the metal ion center in the macrocycle and the terminal groups[13-15]. For example in the case of ZnTPP (Zn-Tetra Phenyl Porphyrin) the molecule is terminated by four phenyl groups[16] and a Zn atom occupies the molecular center, coordinated by four equivalent N atoms. In a thick ZnTPP film the molecules interact by means of weak Van-der-Waals forces, thus maintaining a structure similar to the one they have in the gas phase[17].

ZnTPP isolated molecule is then well understood and in literature many works[18-20] were focused to his adsorption behavior on different substrates.

Here we have studied the hybrid interface of a ZnTPP dye adsorbed in-situ on a nano-tree forest of TiO_2, grown by pulsed laser deposition (PLD) with controlled morphology and structure down to the nanoscale. The study was accomplished by synchrotron radiation electron spectroscopies, in order to gain insight into chemical bonding, electronic properties and charge transfer dynamics between ZnTPP monolayer and the TiO_2 substrate.

Adsorption of ZnTPP on single crystal surfaces was already addressed by STM, XPS, NEXAFS and ResPES experiments, investigating the substrate – molecule interaction, molecular orientation, surface and interface electronic properties, and charge transfer dynamics[18-20]. In particular these studies were performed without the use of any additional linker between the organic molecule and the substrate. The molecule-substrate charge transfer is primarily driven by overlap of orbitals, establishing therefore a strong connection between adsorption geometry (i.e. coupling with the

substrate) and charge injection. In detail, Castellarin-Cudia et al.[19] showed that ZnTPP adsorption orientation was different in case of Si(111) and Ag(110) surfaces. In particular ZnTPP macrocycle and phenyl rings lie flat on the Ag(110) surface while they are rotated (the phenyls almost orthogonal) on Si(111). Consequently the charge transfer dynamics probed by ResPES was much stronger in the case of a ZnTPP monolayer adsorbed on Ag(110), while on Si(111) the ZnTPP monolayer ResPES spectra were more similar to the ZnTPP multilayer ones.

These experiments show the importance of understanding the dye adsorption geometry on the oxide surface. Some works have already addressed more realistic systems of Ru-based dyes on nanoporous TiO_2 even though there were many difficulties related to the ex-situ sample preparation[21]. However, to the best of our knowledge, similar experiments have not been performed for porphyrins on more realistic, nanostructured oxides surfaces, nor the influence of surface oxidation state or chemical modification of the surface was addressed up to now. In fact, even if single crystals represent good model systems since they possess well controlled and reproducible surfaces, molecular interactions with a nanoporous and cluster-assembled oxide can be radically different due to the complex nano-scale surface structure in contact with the molecules (e.g. different active facets, edges, defects at the crystallite boundaries and on the surface, absence of long-range order, sub-stoichiometric sites).

For the mentioned reasons, in this study the ZnTPP adsorption and interface formation was addressed by investigating the properties of a monolayer of molecules on a hierarchical organized ns-TiO_2 substrate. To model different interfaces possibly occurring in a DSSC, the behavior of ZnTPP on surfaces with different oxygen stoichiometry, without changing the overall morphology, was studied. On the basis of our results we propose a scheme for the molecule-substrate coupling and the factors that influence the charge transfer dynamics between the photo excited adsorbate and the oxide surface, which we found to be strongly related to the TiO_2 surface stoichiometry.

2. Experimental

Titanium oxide hierarchically assembled films with a thickness of about 200 nm were grown by PLD on Si substrates at room temperature by ablation of a Ti target (purity 99.99%) with UV ns pulses from a KrF excimer laser (λ=248 nm, pulse duration 10-15 ns, 10 Hz repetition rate); the pulse energy was 300 mJ, corresponding to an energy density (fluence) of about 3 J/cm^2. The deposition was performed in a Ar:O_2 — 4:1 mixture atmosphere at a total pressure of 30 Pa; the target-to-substrate distance was set at 58 mm; the deposition rate was in the range 0.5-1 nm/s.

A post-deposition annealing treatment in air at 400°C was performed for 2 h in a muffle furnace to induce structural ordering (transition from amorphous to anatase phase), as discussed in Di Fonzo et al.[22]. The crystalline structure was checked by means of Raman spectroscopy with a Renishaw InVia spectrometer using the 514.5 nm wavelength of an argon ion laser.

At this stage SEM images were acquired with a Zeiss Supra 40 field emission scanning electron microscope. After preparation, samples were stored in static vacuum. For the synchrotron radiation spectroscopy experiments, as-prepared stoichiometric TiO_2 surfaces were degassed in UHV at 300-350°C for 30 min in order to remove any contaminants and then annealed at 320°C for 60 min in oxygen ($2x10^{-6}$mbar) in order to ensure a good oxidation. The surface stoichiometry was checked by XPS measurements. A defected surfaces, characterized by the presence of a number of Ti^{3+} species associated with oxygen vacancies, was prepared by a further annealing in UHV at 600°C for 15 min and checked by looking at the appearance of a feature at 1eV in the valence band spectra. In both cases, no changes in the anatase structure occur, see supporting information.

High purity (99.95%) commercial ZnTPP (Sigma-Aldrich) was deposited on the TiO_2 samples *in-situ* by a home made evaporator made from Ta. To prepare the monolayer, a thick film was first sublimated in UHV and then annealed at 250°C as described elsewhere[19-20]. This method has proved to form a ZnTPP monolayer on different mono-crystalline substrates. Moreover, the thermal

treatment at 250 °C in UHV does not change the stoichiometry of the substrate, as verified by XPS, see supporting information.

Photoemission measurements were performed at the Material Science (MS) and BACH beamlines at the Elettra synchrotron radiation facility in Trieste[23, 24]. In both end stations NEXAFS and XPS spectra were recorded in normal emission (NE) geometry with the incident beam at 60° relative to the surface normal; in XPS measurements, the overall spectral resolution was between 0.4 and 0.8 eV at ~500 eV photon energy. NEXAFS experiments at the C and N K edges were acquired in Auger Yield mode. In ResPES experiments, valence band spectra were acquired across the C K edge at selected photon energies.

Great care was taken in monitoring beam-induced sample damage such as TiO_2 surface reduction, as already outlined in a previous study on similar samples[25]. Since both ZnTPP and TiO_2 were found to be sensitive to light exposure, we worked using a reduced flux and we continuously checked the integrity of the system by XPS and valence band measurements. In the following we refer to the samples annealed in O_2 as *stoichiometric* TiO_2 while *defective* TiO_2 indicates a sample annealed at 600°C in vacuum.

The core level photoemission spectra were referenced to the Ti $2p_{3/2}$ core level of TiO_2 at 458.8 eV; the C 1*s* multilayer spectrum was fitted by four mixed Gaussian Lorentzian lineshapes (GL), fixing their relative intensity in the ratio 24:8:8:4 to mimic the theoretical carbon bonds present in the ZnTPP (phenyl, pyrrolic C-C-N and C-C-C, meso-bridge C atoms) with the energies of the components reported in Castellarin Cudia et al.[17] as initial values for the fits. Furthermore the FWHM was constrained to be equal for all the components. The GL width and the mixing ratio obtained in the multilayer fit were used as a basis for the monolayer curve fitting analysis, while intensity and position were allowed to vary in a narrow range around the multilayer results. In addition, a few shake up components were introduced to fit the multilayer spectrum well. N 1*s* spectrum was aligned and fitted in a similar way.

The ResPES spectra were collected at the C K-edge of a ZnTPP multilayer, as well as ZnTPP monolayers deposited on a stoichiometric and on a defective TiO_2 surface. All the data were normalized to the substrate Ti 3p peak intensity, moreover in both monolayers the clean TiO_2 substrate signal was subtracted in order to focus on the ZnTPP electronic states' behavior. The energy alignment was done by using the Ti 3p (37.6 eV, BE scale) and Zn 3d lines (10.3 eV, BE scale).

3. Results

3.1 Properties of hierarchically structured TiO_2

PLD in a background atmosphere at the selected Ar:O_2 pressure of 30 Pa results in low energy deposition and TiO_2 cluster nucleation leading to a nanoporous assembly of nanoparticles about 10 nm in size, characterized by a quasi 1-D hierarchically organized assembly of nanoparticles resembling a forest of trees with <0.5 g/cm^3 density and a porosity of about 90%, as discussed by Di Fonzo et al.[22]. A SEM image of the as deposited film is shown in Figure 1a. In a previous work[25] we showed that after thermal annealing in air the nanoparticles possess an anatase crystalline structure; for the investigated sample the crystalline phase was checked by Raman spectroscopy (not shown). Annealing in air at 400°C induces a slight densification, an increase in particle size and an improved inter-particle connection (see Figure 1b), without significantly affecting the mesoscale organization and morphology of the whole assembly.

The stoichiometry of the surface was checked by measuring the Ti 2*p* core levels (see supporting information) and the Valence Band (VB) (Figure 2), showing almost no Ti^{3+} contributions for the best oxidized surface. A well defined defect state is instead seen for the substoichiometric defective samples: see the peak in figure 2e at an energy of about 1 eV near the Fermi edge, attributed to oxygen vacancies[26]. It is evident in Figure 2 that in our samples this feature is almost absent in stoichiometric TiO_2 (Figure 2c) and quite intense in vacuum annealed samples (Figure 2e).

3.2 Properties of ZnTPP/TiO_2 hybrid interfaces

3.2.1 Electronic properties

The valence band spectra of a ZnTPP monolayer deposited on stoichiometric and defective TiO_2 surfaces are shown in Figure 2 in comparison with the clean surfaces and the ZnTPP multilayer.

The lowest energy region (0 – 5 eV) is enlarged and shown in the inset. The spectra are aligned to the Zn 3d level and normalized to the substrate related O 2s feature.

The ZnTPP HOMO in the multilayer case is located at 1.8 eV (Fig. 2a) while the defect state in the defective clean TiO_2 is at 1.1 eV (Fig. 2e). These values are in line with those reported in literature[17,26]. The spectrum of the ZnTPP monolayer on defective TiO_2 shows instead a peak located at ~1.4 eV (Fig. 2d). This peak appears at lower intensity and is slightly wider with respect to the defect state of the clean defective TiO_2 (Fig 2e), this can suggest that the peak at ~1.4 eV is the convolution of the ZnTPP HOMO at ~1.8 eV and the TiO_2 *3d* defect state at 1.1 eV.

The ZnTPP monolayer on stoichiometric TiO_2 (Fig. 2b) shows a small and even wider peak in the range 2eV to 0eV BE. Looking at the spectrum we can assume that also in this case the feature is due to: ZnTPP HOMO located slightly below 2.0 eV and a low intensity TiO_2 defect state at 1.1 eV. The presence of a defect state contribution in the valence band may point to surface reduction following molecular adsorption (see below).

The ZnTPP HOMO is mainly located in the ZnTPP macrocycle, so that if the molecule-substrate interaction is via the phenyl rings, where part of the LUMO states are located, it would not be so evident in the valence band spectrum, which is strongly influenced by the substrate.

Because of this, we also studied the LUMO levels by means of NEXAFS spectroscopy at the N K-edge to get information mainly about the macrocycle, since nitrogen is located there, and at the C K-edge to get information about both the macrocycle and phenyl rings. From the literature[17, 19-20], it is known how to assign the contributions of the different features in the C K-edge NEXAFS spectrum to the different functional groups (macrocycle and phenyls) of the molecule, as also shown below. NEXAFS data are shown in Figure 3.

Figure 3a shows the N K-edge NEXAFS spectra of the analyzed cases: ZnTPP monolayers on stoichiometric and substoichiometric defective TiO_2, and ZnTPP multilayer for comparison. No

difference is observed between the LUMO levels of the multilayer case and the two-monolayer cases, suggesting a weak interaction between the porphyrin macrocycle and the substrates.

Figure 3b shows the NEXAFS spectrum collected at the C K-edge. In the literature[17, 19-20] the first band at 284.1 eV is assigned to transitions to the ZnTPP π* LUMO level which is known to be localized in the macrocycle; the second doublet peak at 285 eV is, instead, mainly due to π* LUMO levels located on the phenyl rings; the remaining 287.3 eV and 288.3 eV peaks are due to σ bonds. Comparing the two monolayer spectra, we observe a difference in relative intensities of the bands. The intensity of transitions to the σ bond increases in the case of stoichiometric TiO_2 surfaces with respect to the π* feature localized on the phenyls, while the spectral lineshape of the monolayer in the case of the defective surface is more similar to the multilayer one. These differences point to an electronic structure change driven by bonding with the substrate, i.e. a molecular electronic state re-arrangement due to direct orbital overlap (σ bond) between the phenyl groups and stoichiometric TiO_2 (orientation effects in this experiment can be neglected because of randomly oriented nanostructured surfaces).

To better analyze the chemical bonding between TiO_2 and ZnTPP, we performed core level spectroscopy by collecting C 1*s* and N 1*s* spectra for each case, as shown in Figure 4, where C 1*s* and N 1*s* photoelectron spectra and their fitted curves are reported.

The spectra in Figure 4a show the C 1*s* data. The multilayer spectrum served as a starting basis for the analysing the monolayer case (experimental part and Castellarin Cudia et al.[17]). At a first glimpse the ZnTPP monolayer on stoichiometric TiO_2 presents an extra feature at 285.8 eV, which was absent in the ZnTPP multilayer. This feature is associated with C-O bonds[27, 28] and thus can indicate a molecule-substrate bond, which involves the substrate oxygen and the carbon of the ZnTPP molecule. The intensity ratio between the other four components is also modified, and deviates from the theoretical multilayer 24:8:8:4 ratio. The total C 1*s* band area was normalized to

the 44 C atoms, and in table 1 we report the average number of carbon atoms per bond found in the different samples. In the case of the ZnTPP monolayer on stoichiometric TiO_2 surfaces, the molecule-substrate bonding feature (2.4 atoms) develops primarily at the expense of the phenyl ring component (21.5 atoms instead of 24). Then, on average, around 2.5 phenyl carbon atoms undergo bonding with the oxidized substrate. The other three molecular components show smaller deviations with respect to the multilayer values. Errors in the best fit are still fairly high, but below the observed variations in the multilayer case.

The bonding is different for the defected substrate. The appearance of the bonding feature at 285.1 eV which can be considered also in this case as a C-O bond, is still observed with a similar intensity (2.6 atoms), but the affected molecular components (see table 1) belong to electrons of the macrocycle (pyrrolic C-C-N and C-C-C, meso-bridges C atoms), while the phenyl component weight seems unchanged by the ZnTPP adsorption and bonding on the defective surfaces. On average, pyrrolic C-C-N and C-C-C bonds and meso-bridge carbon atoms all lower their spectral weight by around 1 atom following the bonding with TiO_2 defective surfaces.

As mentioned above, in addition to the main peaks, the ZnTPP C 1*s* spectra in Figure 4a show shake up components that are also affected by the substrate interaction. In particular it is possible to observe a quenching of these components in the case of the monolayer on quasi stoichiometric TiO_2, compared to the multilayer case, while when adsorption is on the defective surface the shake up region is similar to the multilayer case, although less resolved. This supports the model of different ZnTPP/TiO_2 interaction mechanisms for the two surfaces.

Two components are needed to fit the N 1s region (Figure 4b), with the main peak at 398 eV due to the four ZnTPP equivalent nitrogen atoms[17], and a second one at about 401eV for the multilayer, due to a π-π^* shake up in the case of the ZnTPP multilayer. For the monolayer on the stoichiometric surface, the second peak is slightly shifted by 0.3 eV toward the main peak, and also appears more intense. In the case of the monolayer on the defective surface, this peak is strongly shifted by 0.9 eV

to 400.1 eV with respect to the shake up, so it cannot be associated with the same transition. This component may originate from the contribution of bonds between N and under-coordinated Ti atoms[29]. While the main peak falls essentially at the same binding energy for all the samples, indicating a similar overall chemical environment, the second peak suggests some changes, which are to be explained considering also the C 1*s* spectrum results. A fraction of N atoms (slightly less than one fifth) on the defective surface give clear evidence of the N-under-coordinated Ti bonds, suggesting interaction of the macrocycle core with the substrate surface. On the stoichiometric surface, the second peak can be explained by a superposition of shake-up components (as in the multilayer), and a second peak due again to a (lower) fraction of N atoms interacting with the substrate, although a more precise analysis cannot be done due to the superposition of the lines.

3.2.2 Charge transfer Dynamics

We studied the charge transfer dynamics by performing resonant photoemission spectroscopy experiments[30-33]. This method can be viewed as analogous to a pump and probe technique: a core electron is excited to an empty state followed by a de-excitation process; the created core-hole is characterized by a lifetime which corresponds to a fixed time scale, allowing us to study the charge transfer with respect to this timescale. The de-excitation process gives rise to a resonant spectrum characterized by a normal, a spectator and a Raman participator Auger decay. The intensities of these resonances are measured and information on dynamic charge transfer is obtained because the transferred charge does not contribute to the resonant spectrum, causing an intensity decrease of the resonant features[30-33].

The experiment works in the following way: photon energies across a core level edge are used to excite electrons, and for each excitation energy, a valence band spectrum is collected. The integral of each electron spectrum as a function of photon energy is the NEXAFS spectrum, but each single valence band spectrum allows the determination of the possible charge transfer channels, by

analyzing the changes of the different features forming each spectrum. In the de-excitation process the spatial overlap between the probed excited state and the conduction bands of the hosting substrate affects the balance between the various decay channels. In this way the charge transfer dynamics can be monitored and the core hole lifetime, in the low-fs and sub-fs time regime, represents the timescale[30-33].

From a single ResPES spectrum it is impossible to distinguish whether the excited electron delocalizes to the substrate or to a neighbor atom belonging to the same molecule. As a consequence, in order to distinguish the molecule-molecule from the molecule-substrate delocalization, the ResPES spectra of monolayers are compared to one another and to those obtained on a thick film where only the weak electrostatic molecule-molecule interaction is involved[33]. Furthermore since the photon energy is scanned across a core level threshold, the chemical selectivity of the NEXAFS spectrum applies to ResPES spectroscopy too. In the case of the ResPES C-Kedge spectrum of ZnTPP it is possible to recognize which part of the molecule (phenyls/macrocycle) is interacting with the substrate.

In Figure 5a and 5b the resonant spectra are displayed at selected photon energies across the C K-edge for the two monolayers. Spectral features of both ZnTPP and TiO_2 are present, and the Ti 3p and O 2s features are the most intense, while in the valence band region (11-0 eV) the Zn 3d contribution at 10.3 eV overlaps other molecular components and the TiO_2 substrate derived states. Compared with the valence bands reported above (figure 2) the substrate electronic states are the most intense in this photon energy region.

A spurious peak is also present in the spectra, due to C 1*s* photoelectrons excited by second order light. Unfortunately it overlaps the features due to first order excited valence electrons near the Fermi level, usually the ZnTPP HOMO levels, and hampers the analysis of this energetic region.

From these data, we discern an interesting feature in the shoulder at around 4 eV in the main valence band. This feature is almost absent in the off resonance valence bands (275 eV) and

becomes more intense for photon energies of 284.8, 285.0 and 285.2 eV, while at higher photon energies the shoulder has a lower intensity and its line-shape does not change anymore. This behavior is observed for ZnTPP on both the stoichiometric (Figure 5a) and defective (Figure 5b) substrates.

In order to make a proper analysis of the resonant behavior of this feature a TiO_2 substrate reference spectrum was subtracted from the raw spectra of figure 5, to show only the ZnTPP molecular spectral features.

The data are reported in figure 6 together with resonance valence band spectra acquired on the multilayer ZnTPP thick film. The spectra show the Auger normal and spectator C KVV peak, i.e. the large feature which shifts in binding energy and increases in intensity with changing photon energy, the Zn 3d photoelectrons and the features, labeled A, B, C, D, E, and F, due to molecular orbitals derived form N and C atom electronic states.

These features are particularly evident in the multilayer spectra but, although present, are somewhat difficult to discern in the monolayers due to a lower signal to noise ratio. The intensity change of these features with photon energy gives the part of the resonant spectrum. In case of charge transfer from the molecules to the substrate, these features are quenched with respect to the multilayer case.

In figure 6, interesting differences are observed by comparing the spectra of all three cases. In Figure 6a, the multilayer spectra are characterized by strong resonances corresponding to photon energy ~285.3 eV, assigned to the excitation of C 1*s* electrons belonging to phenyl rings as shown by the NEXAFS spectrum (Figure 3). At that photon energy, several valence band features are reproduced, but in particular we note the state at 4-5 eV, labeled B in Figure 6a, which is particularly pronounced, together with D. This last one can be observed as a shoulder of the Zn 3*d* peak, even if it is not clearly distinguishable because of the increasing Auger signal.

The resonance spectra of the two monolayers are presented in Figure 6b and c: as for the multilayer case, the resonances appear when the C 1*s* of the phenyl rings are excited (range 284.8 - 285.2 eV), however they have different intensity. In particular the B feature has the most recognizable behavior, and the spectra of figure 6b and 6c give an overview of the resonant behavior. Figure 6d presents the spectra of all three cases at the same photon energy, ~285 eV.

It is evident that the B state resonances in the case of monolayer on stoichiometric TiO_2 are quenched with respect to those of the monolayer on defective TiO_2; in the second case the resonances more closely resemble the multilayer case. This different behavior points to a faster dynamic charge transfer (observed lower resonance intensity[30-34]) from the molecule toward the substrate in the case of the ZnTPP monolayer on stoichiometric TiO_2, rather than in the case of defective titania.

Concerning the other valence band features, we observe a similar resonant behavior for the states named D, E, and F. The intensity enhancement happens when phenyl rings are excited and this enhancement is higher when the ZnTPP molecules are bonded to a defective substrate. Similar considerations apply to the resonance of state B, although the resonance of states D, E, F is less strong.

4. Discussion

Formation of a Ti-O-C bond and the effect of chemical differences between TiO_2 substrates has been reported in the literature. However, to our knowledge not many works report investigations of C-O bonding between benzene/phenyl C and TiO_2 oxygen.

The TPP porphyrin phenyl rings are generally 60°-75° rotated with respect to the molecular plane when adsorbed on a surface[19-20, 32-33] and the formation of a Ti-O-C bond, where C belongs to a phenyl ring that does not lie flat on a TiO_2 anatase surface, has been described by Syres et al.[28], who investigated dopamine deposited on TiO_2 anatase. This molecule consists of a phenyl ring with two hydroxyl groups and one ethylamine chain, each of them bonded to one C of the phenyl ring. According to Syres et al. dopamine bonds to the TiO_2 anatase surface through the oxygen atoms in a bidentate geometry and the phenyl ring does not lie flat on the surface, being almost orthogonal to the substrate plane; a Ti-O-C bond is formed. In this case the oxygen belongs to the dopamine molecule instead of being a substrate oxygen, as it replaces missing oxygens forming bonds to an under-coordinated Ti, oxidising it from Ti^{3+} to the Ti^{4+} state. The C-O bond which characterizes this molecule shows a geometry which is very similar to the present system: a C of the phenyl group is bonded to an oxygen surrounded by Ti^{4+} atoms. The authors report a BE of 285.9 eV for the C atoms which form the Ti-O-C bond, which value is quite close to ours.

In a similar manner Syres et al.[34] have also analyzed pyrocatechol (1,2-dihydroxybenzene) on anatase TiO2 (101) and rutile (110) discovering the aromatic ring to be oriented at 27° and 23°, respectively, from the surface normal: this is another example of a benzene ring that does not lie flat on a TiO_2 substrate and the adsorption on the TiO_2 (101) is in bidentate geometry.

Other molecules with no phenyl rings, which form C-O bonds with TiO_2 surfaces, show different C1*s* BEs for the C in the C-O bond. As an example, the value points towards higher binding energies in the case of Ti-O-C bond formed by an alkene chain, as shown by Franking and

Hamers[35]. Actually they report data for alkenes adsorbed on rutile TiO_2 and they located the C1*s* BE of the carbon involved in the Ti-C-O bond at 286.2 eV.

From the fingerprint of C1*s* we confirm the phenyl/substrate interaction and the absence of a macrocycle/substrate interaction in the case of ZnTPP monolayer on stoichiometric TiO_2.

This is in line with the N 1*s* spectrum, which only in the case of defective TiO_2 shows a shoulder at 400.2 eV, which can be attributed to an N-under-coordinated Ti bond. Shao-Chun et al.[29] reported the synthesis of azobenzene via oxidation of anilines and in this case the effect is much more pronounced on defective TiO_2 supports. After dissociation of anilines they locate the N1s energy of nitrogen in the N-Ti bond at ~400.5 eV, which is very close to the value found in our N 1*s* fitting results. This feature suggests the presence of a macrocycle/substrate interaction in our experiment on defective TiO_2. This interaction is not possible for stoichiometric TiO_2 since there are no available electrons to bind to N, while they are present in the case of reduced TiO_2.

Finally looking at the NEXAFS C K-edge spectrum of the ZnTPP monolayer on quasi-stoichiometric TiO_2, a lower intensity of the feature associated with phenyls with respect to the one associated with σ states is observed, suggesting a filling of the LUMO states located on the phenyl ring. Furthermore in the same case the feature associated with the macrocycle at 284 eV is wider comparing to the multilayer case. This could be due to the presence of a second feature at ~283 eV, which could be attributed to a new LUMO state due to the bonding between the phenyl ring and the substrate as observed by Syres at al.[28] in the case of dopamine on anatase. They provide experimental and theoretical evidence of the existence of two new LUMO states at 281.7 eV and 282.8 eV, due to the bonding of the molecule to the titania substrate through a C-O-Ti bond. According to the authors this bond gives rise to a different dynamic charge transfer without an e^- - hole separation in the dye as normally happens in DSSCs.

They suggest a direct photoinjection of the electron from the dopamine to the conduction band of TiO_2. According to them the charge transfer is due to the e^- excitation from the highest occupied π

states of the dopamine to the Ti^{4+} (3d) levels, which are empty in the case of stoichiometric TiO_2. This would explain why the dynamic charge transfer is more favored in the case of stoichiometric TiO_2 than in the case of a defective surface and why it concerns mainly the phenyl rings.

5 Conclusions

In this paper we reported a study of the interaction between nanostructured TiO_2 anatase surfaces and ZnTPP dye molecules. We have shown how the interaction changes, depending on TiO_2 stoichiometry. As a consequence, different charge transfer channels are opened, which lead to different charge transfer mechanisms. In particular the stoichiometric TiO_2 surface favors the bonding of ZnTPP through the phenyl rings, opening a new dynamic charge transfer channel, which allows the excited electron to move directly to the support conduction band. This effect is not equally efficient in the case of ZnTPP on the defective TiO_2 surface. Our approach allowed to deeply investigate the chemical bond between a model dye and nanostructured TiO_2 photoanode surface and to monitor the occurrence of charge transfer. A complete understanding of the complex interaction between organic dyes and oxides in a hybrid interface relevant for photovoltaic applications may help to identify suitable strategies to improve efficiency in a hybrid solar cell device.

Supporting Information Available

X-ray absorption spectra (Ti L_{23} edge) and X-ray photoemission spectra (Ti 2*p* level) of ns-TiO_2 substrates. Effects of thermal treatments are shown. This information is available free of charge via the Internet at http://pubs.acs.org

6. References

[1] Cahen, D.; Hodes, G.; Gratzel, M.; Guillemoles, J. F.; Riess, I. Nature of Photovoltaic Action in Dye-Sensitized Solar Cells**.** *J. Phys. Chem. B* **2000**, *104*, 2053-2059.

[2] Grätzel, M. Dye-Sensitized Solar Cells. *J. Photochem. Photobiol. C: Photochemistry Reviews* **2003**, *4*, 145–153.

[3] Yella, A.; Lee, H; Tsao, H. N.; Yi, C; Chandiran, A. K.; Nazeeruddin, M. K.; Diau, E. W.; Yeh, C.; Zakeeruddin, S. M.; Grätzel, M. Porphyrin-Sensitized Solar Cells with Cobalt (II/III)–Based Redox Electrolyte Exceed 12 Percent Efficiency. *Science* **2011**, *334*, 629-634.

[4] Cho, I. S.; Chen, Z.; Forman, A.J.; Kim, D.R.; Rao, P. M.; Jaramillo, T. F.; Zheng, X. Branched TiO_2 Nanorods for Photoelectrochemical Hydrogen Production. *Nano Lett*. **2011**, *11*, 4978–4984.

[5] Ko, S. H.; Lee, D; Kang, H. W.; Nam, K. H.; Yeo, J. Y.; Hong, S. J.; Grigoropoulos, C. P.; Sung, H.J. Nanoforest of Hydrothermally Grown Hierarchical ZnO Nanowires for a High Efficiency Dye-Sensitized Solar Cell. *Nano Lett.* **2011**, *11*, 666–671.

[6] Zhang, Q.; Dandeneau, C.S.; Zhou, X; Cao, G. ZnO Nanostructures for Dye-Sensitized Solar Cells. *Adv. Mater.* **2009**, *21*, 4087–4108.

[7] Zhang, Q.; Cao, G. Nanostructured Photoelectrodes for Dye-Sensitized Solar Cells. *Nano Today* **2011**, *6*, 91—109.

[8] Sauvage, F.; Di Fonzo, F.; Li Bassi, A.; Casari, C. S.; Russo, V.; Divitini, G.; Ducati, C.; Bottani, C. E.; Comte, P.; Graetzel, M. Hierarchical TiO_2 Photoanode for Dye-Sensitized Solar Cells. *Nano Lett.* **2010**, *10*, 2562–2567.

[9] Divitini, G.; Stenzel, O.; Ghadirzadeh, A.; Guarnera, S.; Russo, V.; Casari, C. S.; Li Bassi, A.; Petrozza, A.; Di Fonzo, F.; Schmidt, V.; et al. Nanoscale Analysis of a Hierarchical Hybrid Solar Cell in 3D. *Adv. Funct. Mater.* **2014**, *24*, 3043–3050.

[10] Passoni, L.; Ghods, F.; Docampo, P.; Abrusci, A.; Martí-Rujas, J.; Ghidelli, M.; Divitini, G.; Ducati, C.; Binda, M.; Guarnera, S.; et al. Hyperbranched Quasi-1D Nanostructures for Solid-State Dye-Sensitized Solar Cells. F. *ACS Nano* **2013,** *7*, 10023-10031.

[11] Hoard, J. L. Some Aspects of Metalloporphyrin Stereochemistry. *Ann. New York Acad. Sci.* **1973**, *206*, 18-31.

[12] Kadish, K. M.; Smith, K. M.; Gillard, R. Eds. *The Porphyrin Handbook*. Academic press, San Diego, **2000**.

[13] Paulat, F.; Lehnert, N. Detailed Assignment of the Magnetic Circular Dichroism and UV−vis Spectra of Five-Coordinate High-Spin Ferric [Fe(TPP)(Cl)]. *Inorg, Chem.* **2008***, 47,* 4963-4976.

[14] Vangberg, T.; Ghosh, A. A First-Principles Quantum Chemical Analysis of the Factors Controlling Ruffling Deformations of Porphyrins:• Insights from the Molecular Structures and Potential Energy Surfaces of Silicon, Phosphorus, Germanium, and Arsenic Porphyrins and of a Peroxidase Compound I Model. *J. Am. Chem. Soc.* **1999***, 121,* 12154-12160.

[15] Poveda, L. A.; Ferro, V. R.; De la Vega, J. M.; Gonzalez-Jonte, R. H. Molecular Modeling of Highly Peripheral Substituted Mg- and Zn-Porphyrins. *Phys.Chem. Chem. Phys.* **2000***, 2,* 4147-4156.

[16] Adler, A. D.; Longo, F. R.; Finarelli, J. D.; Goldmacher, J.; Assour, J. Korsakoff, L. A Simplified Synthesis for Meso-Tetraphenylporphine. *J. Org. Chem.* **1967**, *32*, 476.

[17] Castellarin Cudia, C.; Vilmercati, P.; Larciprete, R.; Cepek, C.; Zampieri, G.; Sangaletti, L.; Pagliara, S.; Verdini, A.; Cossaro, A.; Floreano, L.; et al. Electronic Structure and Molecular Orientation of a Zn-Tetra-Phenyl Porphyrin Multilayer on Si(1 1 1). *Surf. Sci.* **2006***, 600*, 4013–4017.

[18] Yoshimoto, S.; Tsutsumi, S.; Suto, K.; Honda, Y.; Itaya, K. Molecular Assemblies and Redox Reactions of Zinc(II) Tetraphenylporphyrin and Zinc(II) Phthalocyanine on Au(1 1 1) Single Crystal Surface at Electrochemical Interface. *Chem. Phys.* **2005,** *319,* 147-148.

[19] Castellarin-Cudia, C.; Borghetti, P.; Di Santo, G.; Fanetti, M.; Larciprete, R.; Cepek, C.; Vilmercati, P.; Sangaletti, L.; Verdini, A.; Cossaro, A.; et al. Substrate Influence for the Zn-Tetraphenyl-Porphyrin Adsorption Geometry and the Interface-Induced Electron Transfer. *Chem. Phys. Chem.* **2010**, *11*, 2248 – 2255.

[20] Vilmercati, P.; Castellarin-Cudia, C.; Gebauer, R.; Ghosh, P.; Lizzit, S.; Petaccia, L.; Cepek, C.; Larciprete, R.; Verdini, A.; Floreano, L.; et al. Mesoscopic Donor−Acceptor Multilayer by Ultrahigh-Vacuum Codeposition of Zn-Tetraphenyl-Porphyrin and C_{70}. *Am. Chem. Soc.* **2009,** *131,* 644–652.

[21] Schwanitz, K.; Weiler, U.; Hunger, R.; Mayer, T.; Jaegermann W. Synchrotron-Induced Photoelectron Spectroscopy of the Dye-Sensitized Nanocrystalline TiO_2/Electrolyte Interface:• Band Gap States and Their Interaction with Dye and Solvent Molecules. *J. Phys. Chem. C* **2007**, *111*, 849-854.

[22] Di Fonzo, F.; Casari, C. S.; Russo, V.; Brunella, M. F.; Li Bassi, A.; Bottani C. E. Hierarchically Organized Nanostructured TiO_2 for Photocatalysis Applications. *Nanotechnology* **2009**, *20*, 015604.

[23] Vasina, R.; Kolarik, V.; Dolezel, P.; Mynar, M.; Vondracek, M.; Chab, V.; Slezak, J.; Comicioli, C.; Prince, K. C. Mechanical Design Aspects of a Soft X-ray Plane Grating Monochromator. *Nucl. Instrum. Methods Phys. Res. A* **2001**, *467- 468*, 561- 564.

[24] Zangrando, M.; Zacchigna, M.; Finazzi, M.; Cocco, D.; Rochow, R.; Parmigiani, F. Polarized High-Brilliance and High-Resolution Soft X-ray Source at ELETTRA: The Performance of Beamline BACH. *Rev. Sci. Instrum.* **2004,** *75*, 1.

[25] Fusi, M.; Maccallini, E.; Caruso, T.; Casari, C. S.; Li Bassi, A.; Bottani, C. E.; Rudolf, P.; Prince, K. C.; Agostino R. G. Surface Electronic and Structural Properties of Nanostructured Titanium Oxide Grown by Pulsed Laser Deposition. *Surf. Sci.* **2011**, *605*, 333–340.

[26] Diebold, U. The Surface Science of Titanium Dioxide. *Surf. Sci. Rep.* **2003**, *48*, 53-229.

[27] Mc Cafferty, E.; Wightman, J. P. Determination of the Concentration of Surface Hydroxyl Groups on Metal Oxide Films by a Quantitative XPS Method. *Surf. Interface Anal.* **1998**, *26*, 549–564.

[28] Syres, K. L.; Thomas, A.; Bondino, F.; Malvestuto, M.; Graetzel, M. Dopamine Adsorption on Anatase TiO_2(101): A Photoemission and NEXAFS Spectroscopy Study. *Langmuir* **2010**, *26*, 14548-14555.

[29] Li, S. C.; Diebold, U. Reactivity of TiO_2 Rutile and Anatase Surfaces toward Nitroaromatics. *J. Am. Chem. Soc*. **2010**, *132*, 64-66.

[30] Brühwiler, P. A.; Karis, O.; Martensson, N. Charge-Transfer Dynamics Studied Using Resonant Core Spectroscopies. *Rev. Mod. Physics* **2002**, *74*, 703.

[31] Schnadt, J.; Brühwiler, P. A.; Patthey, L.; O'Shea, J. N.; Soedergren, S.; Odelius, M.; Ahuja, R.; Karis, O.; Baessler, M.; Persson, P.; et al. Experimental Evidence for Sub-3-fs Charge Transfer from an Aromatic Adsorbate to a Semiconductor. *Nature* **2002**, *418*, 620.

[32] Vilmercati, P.; Cvetko, D.; Cossaro, A.; Morgante, A. Heterostructured Organic Interfaces Probed by Resonant Photoemission. *Surf. Sci.* **2009**, *603*, 1542-1556.

[33] Vilmercati, P.; Castellarin-Cudia, C.; Larciprete, R.; Cepek, C.; Zampieri, G.; Sangaletti, L.; Pagliara, S.; Verdini, A.; Battocchio, C.; Polzonetti, G.; et al. Molecular Orientations, Electronic Properties and Charge Transfer Timescale in a Zn-Porphyrin/C_{70} Donor–Acceptor Complex for Solar Cells. *Surf. Sci.* **2006**, *600*, 4018-4023.

[34] Syres, K. L.; Thomas, A. G.; Flavell, W. R.; Spencer, B. F.; Bondino, F.; Malvestuto, M.; Preobrajenski, A.; Graẗzel, M. Adsorbate-Induced Modification of Surface Electronic Structure: Pyrocatechol Adsorption on the Anatase TiO_2 (101) and Rutile TiO_2 (110) Surfaces. *J. Phys. Chem. C* **2012,** 116, 23515−23525.

[35] Franking, R.; Hamers, R. J. Ultraviolet-Induced Grafting of Alkenes to TiO_2 Surfaces: Controlling Multilayer Formation. *J. Phys. Chem. C* **2011**, *115*, 17102-17110.

TABLES

$ZnTPP/TiO_2$	Multilayer	Monolayer	Monolayer on defective TiO_2
Components	Number of Atoms	Number of Atoms	Number of Atoms
Phenyl ring	24	21,5±1,1	24,5±0,6
Pyrrolic C-C-N	8	8,4±0,7	7,0±0,2
Pyrrolic C-C-C	8	8,4±1,1	7,0±0,2
C meso-bridge	4	3,3±0,7	2,8±0,1
C-O bond		2,4±0,7	2,6±1,0

Table 1. Carbon bonds within the $ZnTPP/TiO_2$ systems, the total number of carbon atoms was fixed at 44.

FIGURES

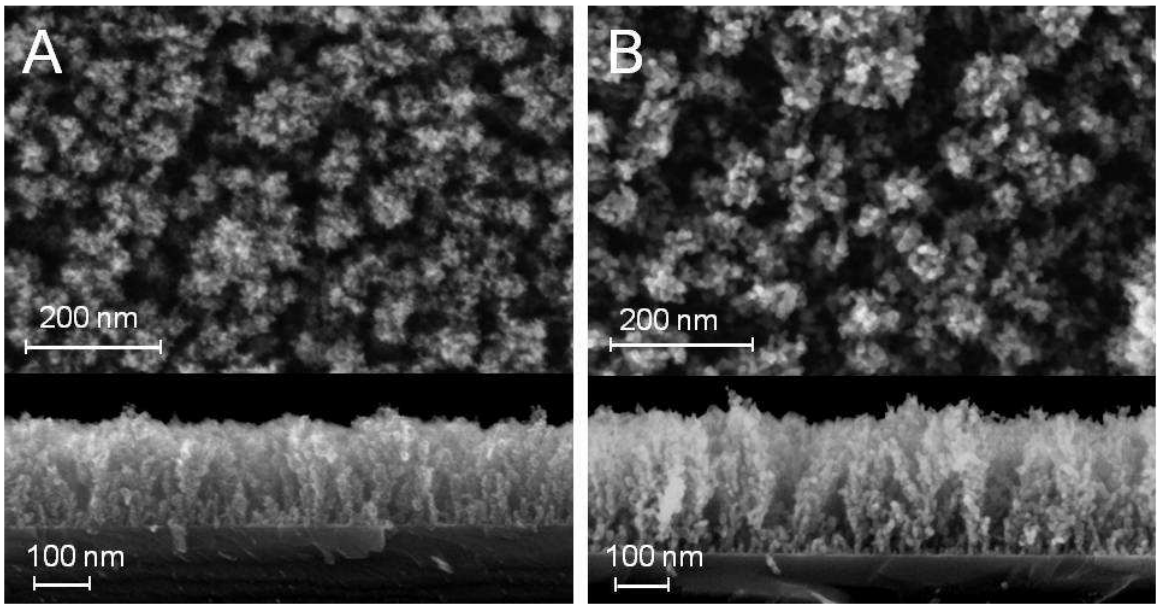

Figure 1. SEM pictures of as deposited (A) and annealed (B) TiO_2 substrates.

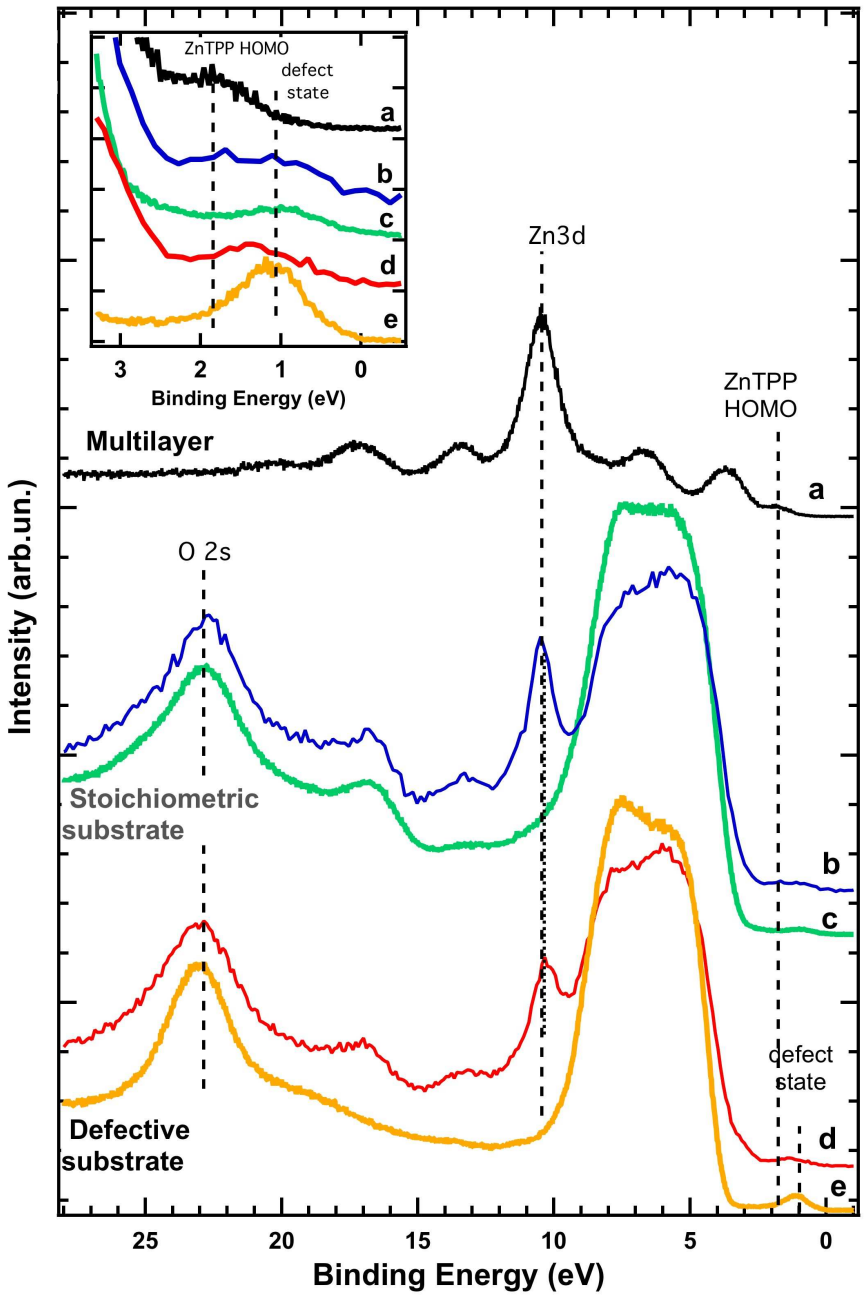

Figure 2. Valence band spectra (photon energy 170 eV) of **a)** ZnTPP multilayer (black), **b)** ZnTPP monolayer on stoichiometric TiO_2 (blue) **c)** clean stoichiometric TiO_2 (green), **d)** ZnTPP monolayer on defective TiO_2 (red) and **e)** clean defective TiO_2 (orange). In the inset, an enlargement of the region 0-4 eV is shown.

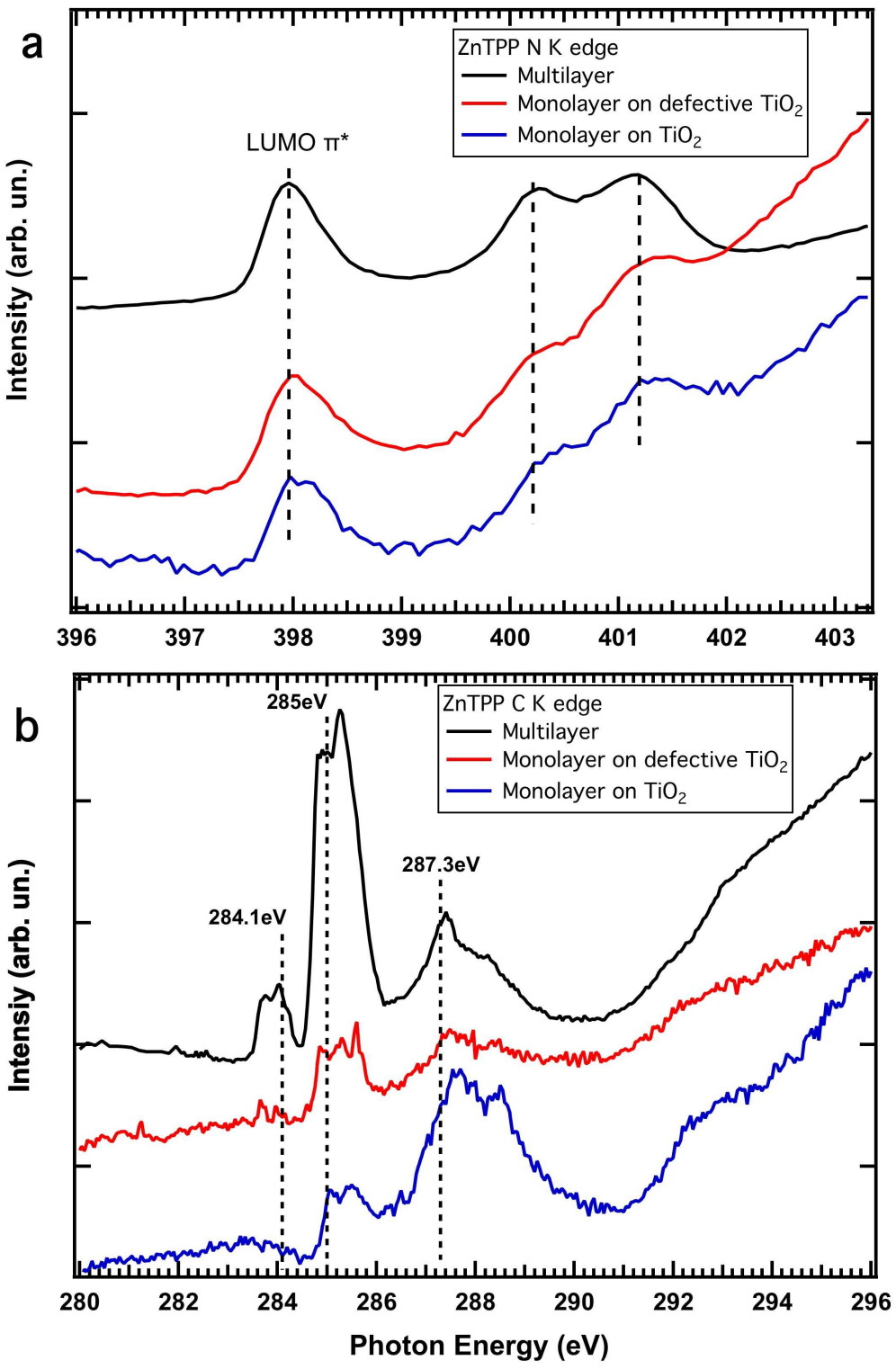

Figure 3: NEXAFS spectra, **a)** N-Kedge, **b)** C-Kedge. Dashed lines are a guide for the eye.

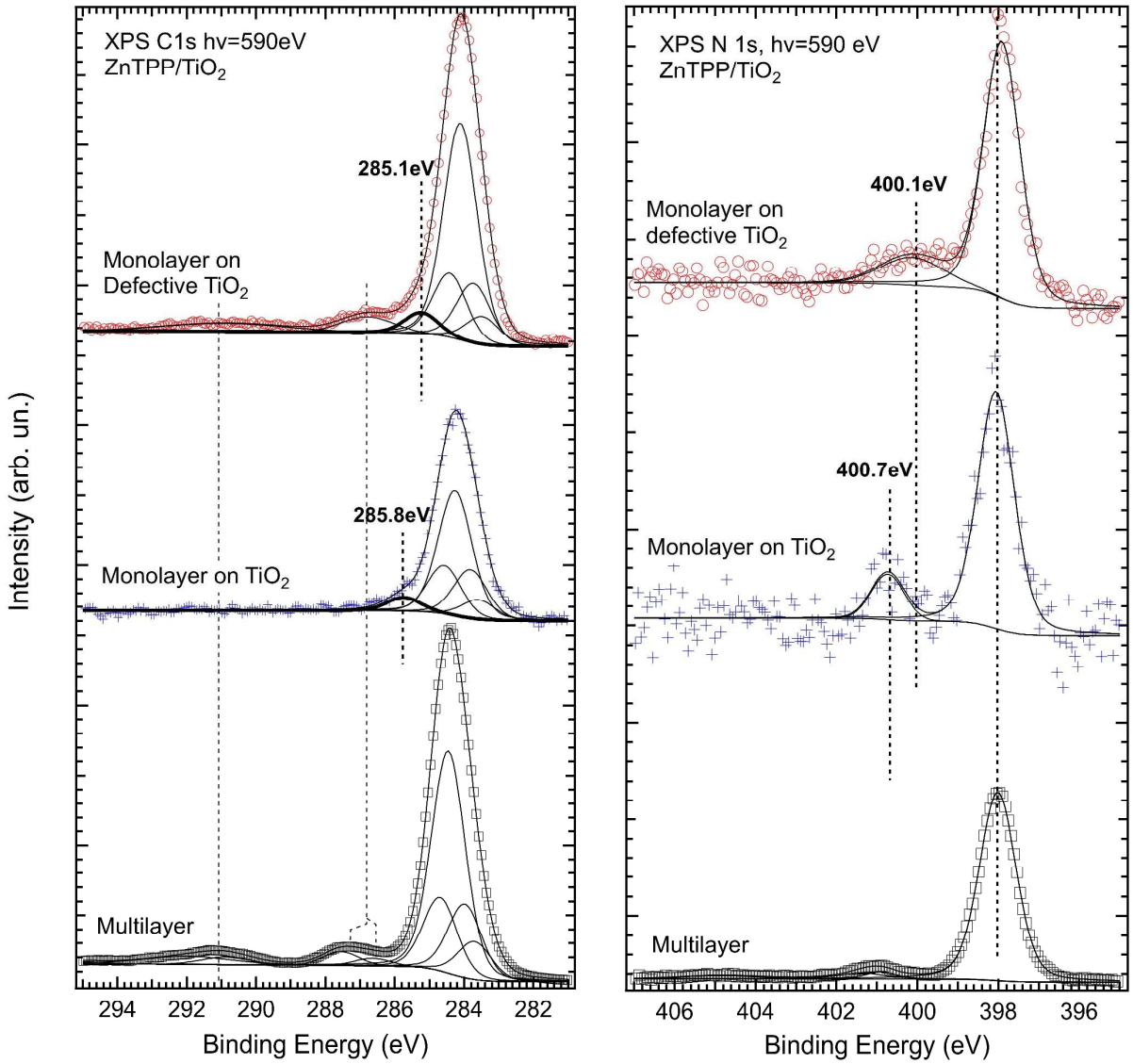

Figure 4. **(a)** C 1s and **(b)** N 1s core level photoelectron spectra from ZnTPP adsorbed on PLD TiO_2 films. Spectra are shown for a ZnTPP thick multilayer, ZnTPP monolayer on pristine TiO_2 surfaces and a ZnTPP monolayer on a TiO_2 defective surface. The best fitting curve are shown for each spectrum.

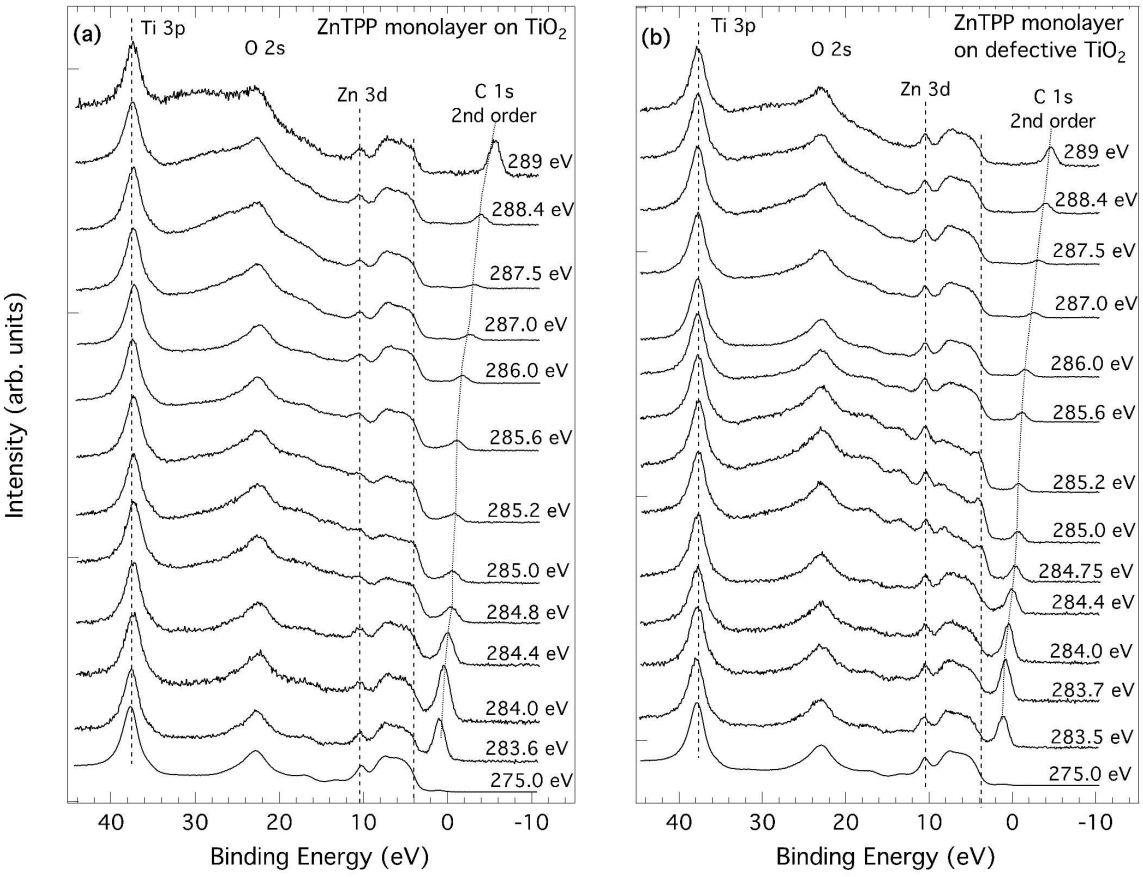

Figure 5: Resonant valence band photoemission raw spectra. **(a)**: ZnTPP monolayer on stoichiometric TiO_2. **(b)**: ZnTPP monolayer on defective TiO_2. Note that the intensity of second order radiation, exciting the C 1s electrons, is not constant relative to the first order light exciting the valence band states.

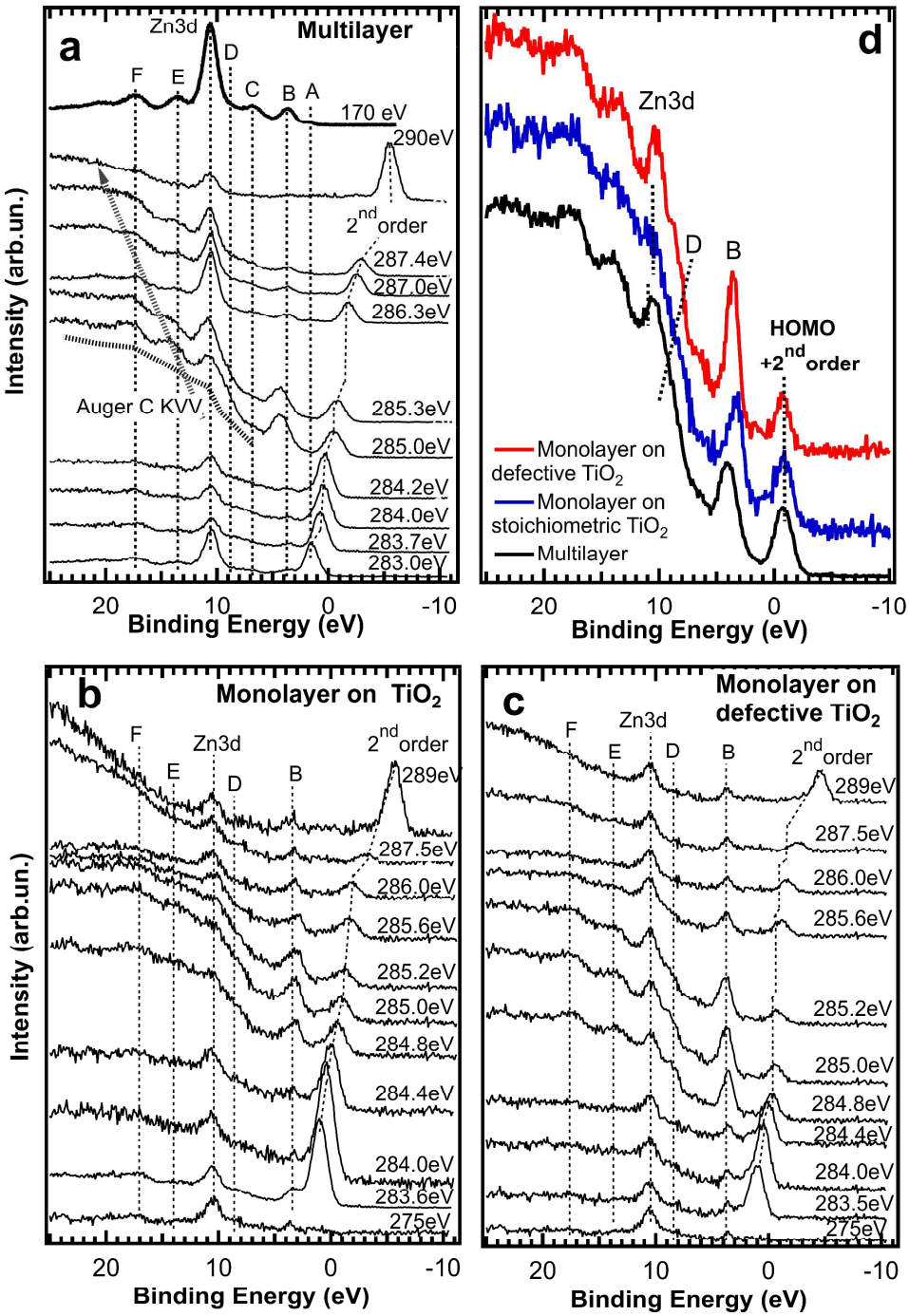

Figure 6: Resonant valence band photoemission spectra. Substrate signal was subtracted from the monolayer spectra reported in fig. 5. **a)** multilayer, **b)** ZnTPP monolayer on stoichiometric TiO_2, **c)** ZnTPP monolayer on defective TiO_2, **d)** VB spectra measured at hν ~285.0 eV for the cases a), b), c)

Table of Contents Graphic